THE JOURNAL OF PHYSICAL CHEMISTRY B

Article

pubs.acs.org/JPCB

Single-Walled Carbon Nanotubes Do Not Pierce Aqueous Phospholipid Bilayers at Low Salt Concentration

Liu Shi, Dachuan Shi, Matthias U. Nollert, Daniel E. Resasco, and Alberto Striolo*

The University of Oklahoma School of Chemical, Biological and Materials Engineering, Norman, Oklahoma 73019, United States

Supporting Information

ABSTRACT: Because of their unique physical, chemical, and electrical properties, carbon nanotubes are an attractive material for many potential applications. Their interactions with biological entities are, however, not yet completely understood. To fill this knowledge gap, we present experimental results for aqueous systems containing single-walled carbon nanotubes and phospholipid membranes, prepared in the form of liposomes. Our results suggest that dispersed single-walled carbon nanotubes, instead of piercing the liposome membranes, adsorb on them at low ionic strength. Transmission electron microscopy and dye-leakage experiments show that the liposomes remain for the most part intact in the presence of the nanotubes. Further, the liposomes are found to stabilize carbon nanotube dispersions when the surfactant sodium dodecylbenezenesulfonate is present at low concentrations. Quantifying the interactions between carbon nanotubes and phospholipid membranes could not only shed light on potential nanotubes cytotoxicity but also open up new research venues for their use in controlled drug delivery and/or gene and cancer therapy.

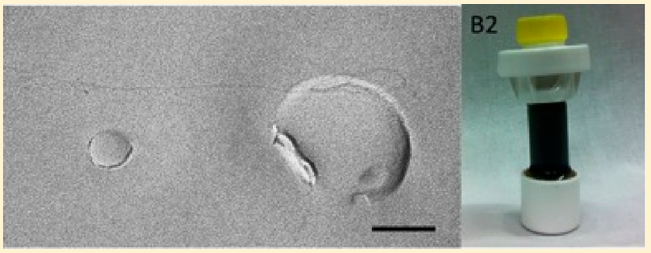

1. INTRODUCTION

Carbon nanotubes (CNTs), members of the carbon allotropes family, are cylinders of graphene sheets. Single-walled carbon nanotubes (SWNTs) have typical diameters in the range of 0.4−2.0 nm and lengths of up to a few micrometers; multiwalled carbon nanotubes (MWNTs) are generally characterized by larger diameters and can reach longer lengths. CNTs exhibit unique physical, chemical, and electrical properties that make them attractive materials for electronic, medical, and other applications.[1,2] Experimental data suggest that CNTs can deliver drugs, antigens, and genes into both prokaryotic and mammalian cells.[3−8] CNTs translocate the plasma membrane of human cell lines such as HeLa and epithelial carcinoma cells.[9,10]

The early enthusiasm for using CNTs in medical applications was mitigated by reports on their cytotoxicity.[11−14] Lam et al., for example, conducted experiments in vivo and found that pristine hydrophobic CNTs accumulated in the lungs of rats, and possibly caused granulomas.[13] The results were, however, difficult to generalize because details regarding CNTs preparation,[14−16] cell type, and culture conditions varied.[8,9] Crouzier et al.[17] reported that purifying SWNTs significantly reduces the lytic effect on red blood cells. Kang et al.[18] assessed the antibacterial effects of well-purified and characterized CNTs toward *Escherichia coli* and found that SWNTs were much more toxic than MWNTs. Vecitis et al.[19] reported that the cytotoxicity toward *Escherichia coli* increased with the fraction of metallic SWNTs.

Experiments also suggested that the type of CNTs functionalization affects cellular uptake, maybe even changing the uptake mechanism.[7,20,21] Although chemical functionalization appeared to alleviate the cytotoxicity of CNTs, surfactants may not provide such a benefit. For example, Liu et al.[22] studied the cytotoxicity of SWNTs to bacteria. They dispersed SWNTs using both the nonionic surfactant Tween 20 and the anionic surfactant sodium cholate (SC). Tween 20 was found not to be cytotoxic, while SC was found to decrease the bacteria survival rate.

The results summarized above suggest that significant progress is being made in understanding the CNTs cytotoxicity. On the other hand, the mechanisms and pathways followed by CNTs entering cells are not clear. The two most likely uptake pathways are endocytosis and direct insertion through the lipid bilayer of the cell membranes. The endocytosis can be either active (ATP driven) or passive (not involving the cell machinery).[23] In an attempt to discriminate between these two possibilities in a model system, experimental data quantifying the interactions between CNTs and phospholipid membranes, perhaps in the form of liposomes, are needed. Although it is recognized that liposomes lack the complexity of cellular membranes, liposomes and synthetic phospholipid bilayer vesicles, as well as supported phospholipid membranes, have been widely used to mimic of cellular membranes in biochemical research.[24−26] For example, Karchemski et al. found that surface-functionalized CNTs could conjugate to liposomes by an amide bond with L-α-phosphatidylethanol-

Received: April 20, 2013
Revised: May 3, 2013

   dx.doi.org/10.1021/jp4039336 | J. Phys. Chem. B XXXX, XXX, XXX−XXX

amine.[27] Posner and his group investigated the partition of fullerenes, as well as that of functionalized gold nanoparticles, between water and supported bilayers.[24,25] Experimental observations can be interpreted with the aid of theory and simulations. Wallace and Sansom,[28] e.g., simulated one CNT as it moved at constant velocity across a lipid bilayer and found that as the CNT pierced the membranes it extracted lipid molecules from it. Hofinger et al.[29] simulated CNTs embedded in phospholipid bilayers. When the CNTs were short (length of 2 nm), they aligned parallel to the lipid molecules (perpendicular to the membrane), but as the nanotube length increased, the CNTs preferentially placed parallel to the membrane. Parthasarathy et al. documented how short SWNTs embedded in phospholipid bilayers affect the structure of lipid molecules.[30]

To complement the existing literature, we present here experiments conducted to document the interactions between well-characterized SWNTs and phospholipid membranes, prepared in the form of liposomes. Liposomes are considered as a minimal model for cellular membranes in which only direct insertion of SWNTs or passive endocytosis mechanisms are possible. The SWNTs were stabilized in aqueous dispersions using the surfactant sodium dodecylbenzenesulfonate (SDBS). Because SDBS is effective at stabilizing aqueous dispersions of SWNTs at low ionic strength, our experiments were conducted at such conditions. The SWNTs employed in this work were of high quality, and carefully characterized. We seek to answer the question: is it possible that SWNTs, dispersed in aqueous solutions at low ionic strength, adsorb into phospholipid membranes and eventually disrupt them?

2. EXPERIMENTAL PROCEDURES

2.1. Materials. High-purity SWNTs [CNT > 98%, SWNT 80−95%, (6,5) SWNT 30−40%] were provided by SouthWest Nanotechonologies, Inc. (SWeNT) (batch # SG 65EX-410). Residual catalysts and other large particles in the sample were removed during the dispersion treatment.[31,32] The average diameter of the SWNTs present in the samples used for our experiments is ∼0.8 nm, estimated based on chirality measurement (NS2 nanospectralyzer), the results of which are consistent with data provided by the producer, SWeNT. The median length of the nanotubes was ∼1.5 μm, as characterized by the manufacturer using the AFM method.

Egg L-α-phosphatidylcholine (egg-PC) and cholesterol were purchased from Avanti Polar Lipids Inc. (purity >99%). Calcein dye and sodium dodecylbenzenesulfonate (SDBS) (purity >98%) were purchased from Sigma-Aldrich and Tokyo Kasei Kogyo Co. Ltd., respectively.

Sephadex-25 desalt columns (HiTrap) were purchased from GE Healthcare. Dialysis membranes with the molecular weight cutoff of 8000−10 000 Da were obtained from Spectrum Laboratories Inc. 18.2 MΩ·cm resistivity water was used for all applications in this work. All other chemicals were obtained from Sigma-Aldrich.

2.2. Preparation of Liposome Suspensions. The liposome suspensions for dialysis were prepared using egg L-α-phosphatidylcholine (egg-PC) and cholesterol. PC was chosen because it is the major component of biological membranes. Cholesterol was used to increase the stability of the phospholipid bilayer. The liposomes were prepared following a sonication method,[32−34] according to which 20 mg of egg-PC and 2 mg of cholesterol were mixed with 5 mg of chloroform in a glass tube. The chloroform was removed under a nitrogen stream at ambient temperature to obtain a dry film of the lipid mixture. The dry film was kept under vacuum to avoid oxidation, as well as to further remove chloroform and other impurities. Prior to use, the dry lipid film was hydrated with 22 mL of water for 30 min, followed by 30 min sonication using a horn sonic dismembrator at 25% power output (Model 500, Fisher Scientific). The 1 mg/mL liposome suspension was extruded 10 times through a polycarbon membrane with pore size of 400 nm (Avanti Polar Lipids Inc.) at ambient temperature to obtain the liposome suspension.

2.3. Preparation of SWNT Dispersions. SWNTs were dispersed in water using the sonication method proposed by Tan and Resasco.[35] Five milligrams of SWNTs and 125 mg of sodium dodecylbenzenesulfonate (SDBS) were added to 25 mL of water in a 95 mL vial. The aqueous system was sonicated for 1 h with a horn sonic dismembrator at 25% power output (Model 500, Fisher Scientific). The suspension was then centrifuged in an automatic centrifuge (Centrifuge 5424, Eppendorf) at 15 000 rpm for 30 min. The upper supernatant dispersion was collected and further processed with a second cycle of sonication and centrifugation. The upper supernatant dispersion collected after the second centrifugation was used within 2 weeks after preparation as the SWNT dispersion for our experiments.

2.4. Dialysis. We removed SDBS from various samples by dialysis to minimize the effects of surfactants on liposomes, and therefore to study exclusively the interactions between liposomes and pristine SWNTs. Several dialysis experiments were conducted, including (a) those for suspensions containing both liposomes and SWNTs (LIPO+SWNT); (b) those for suspensions containing water and SWNTs (W+SWNT); and (c) those for suspensions containing water and 5 mg/mL SDBS (W+SDBS). The aqueous dispersion of 5 mg/mL of SDBS was used as control, because the SWNT dispersions were prepared using the same SDBS concentration. The suspensions used in dialysis experiments were produced by combining a 1:1 volume ratio of the two systems used (e.g., the W+SWNT suspension was prepared by mixing 1 mL of water and 1 mL of SWNT dispersion). A fourth set of experiments was conducted by mixing the liposome suspension and the SWNT dispersion at the volume ratio of 4:1 (4_LIPO+SWNT).

Two milliliters of the various suspensions (LIPO+SWNT, W+SWNT, and W+SDBS) were dialyzed through a dialysis membrane (hydrophilic cellulose ester membrane, purchased from Spectrum Laboratories Inc.) in 200 mL of water, under gentle shaking. In the case of the 4_LIPO+SWNT suspension, only 1.25 mL was used, instead of 2 mL, all other parameters being equal.

The molecular weight cutoff of the dialysis membrane was 8000−10 000, large enough to allow SDBS to diffuse across the membrane while preventing the transport of both SWNTs and liposomes.

During the dialysis experiment, the SDBS concentration in the bulk water was monitored by UV−vis spectrophotometer (UV-2450PC, Shimadzu) at the wavelength of 223 nm. The SDBS concentration can be calculated as a function of time from the absorbance intensity. By knowing the initial SDBS concentration inside the dialysis membrane, the liquid volume within the dialysis cell, the liquid volume of the bulk water out of the dialysis cell, and the change of SDBS concentration in the bulk water out of the cell during the experiment, we calculated the SDBS concentrations inside the dialysis cell. The

dx.doi.org/10.1021/jp4039336 | J. Phys. Chem. B XXXX, XXX, XXX−XXX

stability of SWNT dispersion was monitored as a function of SDBS concentration.

2.5. Dye-Leakage Experiments. To monitor the disruption of liposomes, we conducted leakage measurements by encapsulating a fluorescent dye (calcein) within liposomes. A 2.5 mL chloroform solution containing 10 mg of egg-PC and 1 mg of cholesterol was mixed in a 10 mL round-bottom flask. Chloroform was then removed at ambient temperature using a nitrogen stream, while forming a dry film of lipid mixture. The dry film was kept in a vacuum chamber and before use it was hydrated with 2 mL of 40 mM aqueous calcein solution for 30 min. The calcein aqueous solution was adjusted to pH ∼ 7.4 by adding sodium hydroxide before being used. The resultant suspension was vortexed for 3 min and then subjected through five cycles of freeze/thaw by using liquid nitrogen and warm water. In between each cycle, the sample was sonicated using a bath sonicator (model 08855-10, Cole Parmer) for 1 min. After the five freeze/thaw cycles, the liposome suspension was extruded 10 times through a polycarbon membrane with pore size of 400 nm at ambient temperature. The calcein not trapped within the liposomes was removed by eluting through a size-exclusion Sephadex G-25 column. The liposome suspension collected from the exclusion column was diluted 10-fold in water prior to conducting the dye-leakage experiments.

Calcein leakage from the liposomes was monitored by recording the increase of fluorescence intensity at 528 nm (excitation at 495 nm, slit width of 20 nm) using a plate reader (Synergy HT, Bio-Tek). We measured fluorescence readings after adding 5 μL of reagent to 300 μL of liposome suspension. Pure water, 0.2% Triton X-100 (polyoxyethylene 10 isoctylphenyl ether) in aqueous solutions, SDBS in aqueous solutions, SWNT dispersions, and SWNT dispersions with a low SDBS concentration were used as additions. The SWNT dispersion with low SDBS concentration was obtained by a 3-day dialysis of 2 mL of W+SWNT sample in 200 mL of water to remove SDBS. Triton X-100 was chosen to conduct a control experiment because this surfactant is known to disrupt phospholipid bilayers, causing significant calcein leakage.[34]

To calibrate the calcein leakage results, we used two test experiments. The first was expected to show no leakage, and the second was expected to show maximum leakage. In the first experiment, 300 μL of the liposome suspension was added to 5 μL of pure water. The results showed no change of fluorescence intensity within 4 min. The corresponding fluorescence was used to define the 0% leakage baseline. Complete liposome disruption was achieved by adding 5 μL of the 0.2% Triton X-100 aqueous system to 300 μL of the liposome suspension. The fluorescence reading intensity after 4 min was used to benchmark "100% leakage". The leakage readings obtained during other experiments are reported below as "% leakage", which is the fraction of the total leakage compared to that caused by Triton X-100.

To complete the dye-leakage study, we designed another experiment. In the first step, we combined the liposomes containing calcein and SWNT dispersion with a volume ratio of 9:1. We used this system in a dialysis experiment. The resultant liposome−SWNT suspension on the fourth day of dialysis was collected for a dye-leakage experiment. Triton X-100 was added to this suspension. Leakage from this experiment would indicate that the interactions between SWNTs and liposomes during dialysis do not disrupt the phospholipid bilayers. No change in measured fluorescence intensity from this experiment would indicate that the SWNTs perturb significantly the liposomes during dialysis. The results are discussed below.

2.6. Characterization Techniques. Dynamic light scattering (DLS) was employed to estimate the hydrodynamic size and the zeta potential of liposomes in water (BrookHaven ZetaPALS). Transmission electron microscopy (TEM) with negative stain was used to visualize liposomes in water. Lacey carbon copper TEM grids (Electron Microscopy Sciences) were used to adsorb liposomes from the liposome suspension. The liposome samples were then stained in 2% uranyl acetate aqueous solution for 30 s and dried at room temperature. The specimens were observed on a JEOL JEM-2000FX instrument with an accelerating voltage of 200 kV.

SWNTs were characterized by UV−vis (UV-2450PC, Shimadzu) and Raman spectroscopies (JY Horiba LabRam 800). The Raman spectrum was obtained using dry SWNTs after sonication. To prevent interference, excess SDBS was removed by a 4-day dialysis. Near-IR fluorescence spectra were measured with a NS2 nanospectralyzer (Applied Nano-Fluorescence, Houston, TX) to determine the dispersion quality of SWNT dispersions. The results were obtained using 532 and 783 nm diode laser excitations. Note that spectral analyzer characterization is able to detect all chiralities present in a nanotube dispersion, while Raman spectroscopy is sensitive only to those nanotubes whose transition energy is in resonance with the laser.[36,37]

Freeze-fracture TEM was used to visualize systems composed by liposomes and SWNTs in water. The samples used for these experiments were LIPO+SWNT on the fourth day of dialysis. Freeze-fracture samples were prepared by plunging the sample into a liquid Freon 22 bath cooled by liquid nitrogen. This process is expected to vitrify water in the sample. The samples were then fractured in vacuum with a microtome. The fractured samples were replicated with approximately 5 nm platinum deposition at a 45° angle, followed by ∼100 nm carbon deposition normal to the surface. The replicas were first washed with ethanol 3 times and then dissolved in chromic acid (50% sulfuric acid, 10% sodium dichromate, and water) at ambient temperature. After about 24 h, the replicas were washed in distilled water 3 times to remove residual impurities before being collected on copper TEM grids (Electron Microscopy Sciences). The specimens were then analyzed using a JEOL JEM-2000FX instrument with an accelerating voltage of 200 kV.

3. RESULTS

3.1. Liposome Suspensions. All liposomes were prepared using egg-PC and cholesterol, as described above. One picture of one liposome suspension used in our experiments is shown in Figure 1A, which exhibits the opalescence characteristic of liposome suspensions. Because the liposomes are expected to be roughly spherical, DLS was used to estimate their size. The results show that the average hydrodynamic diameter of the liposomes obtained by sonication method is ∼150 ± 40 nm. Similar hydrodynamic radius was obtained for the liposomes made from the freeze−thaw method. Representative DLS data are reported in Figure S1 of the Supporting Information. By comparison, we point out that the median length of the nanotubes used for our experiments, according to the manufacturer, was ∼1.5 μm, before sonication.

In Figure 1B we report a TEM image of liposomes obtained using the negative stain method. The diameters of the liposomes observed in TEM images are consistent with the

dx.doi.org/10.1021/jp4039336 | J. Phys. Chem. B XXXX, XXX, XXX−XXX

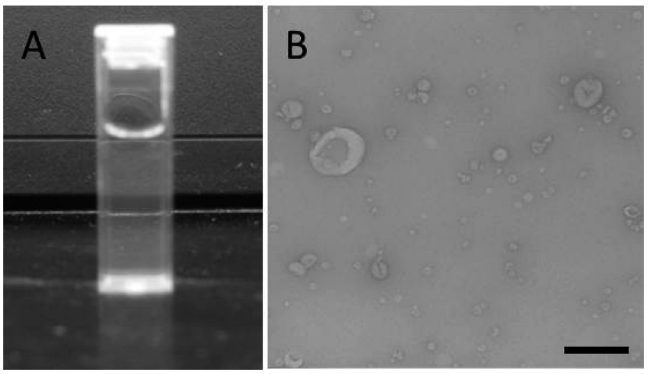

Figure 1. Image of one sample containing a liposome suspension as prepared by the sonication method (A). TEM image of liposomes as obtained with the negative stain method (B). The scale bar in panel B is of size 200 nm.

estimates from DLS experiments, although a wide range of diameters are observed, from ∼20 nm up to ∼400 nm. Visual inspection of several TEM images suggests that in our samples liposomes larger than 200 nm are very few. According to literature, the liposomes of diameter 200 nm or less should be for the most part unilamellar liposomes.[26] Additional TEM images for our liposomes, in some cases with CNTs, are provided as Figure S2 in the Supporting Information.

We measured the zeta potential of egg-PC liposome without calcein as −23.3 ± 1.6 mV, indicating that the liposome membranes are negatively charged, as expected. The zeta potential measured for the liposomes containing calcein was −43.3 ± 5.7 mV.

3.2. SWNT Dispersions. One picture of an aqueous dispersion containing SWNTs stabilized by SDBS is shown in Figure 2A. On the basis of literature observations, we expect that most of the SWNTs in the dispersion are either individually dispersed or in small bundles.[35] Fluorescence spectra (discussed below) obtained for aqueous (6,5) SWNTs dispersed using SDBS demonstrate that this is indeed the case, as bundled SWNTs do not fluoresce.[38−40] The SWNTs dispersions used here were found to be stable for as long as 2 months. For consistency and to ensure high dispersion quality, all the SWNTs dispersions were used within 2 weeks after preparation.

One representative Raman spectrum obtained from the dry SWNTs after sonication is reported in Figure 2B. Raman spectroscopy is typically employed to evaluate the quality of SWNTs (i.e., to estimate the presence of defects) based on the intense G band centered below ∼1600 cm^{-1}, typical of sp2 carbon atoms, and on the weaker D band centered at ∼1300 cm^{-1}, typical of sp3 carbon atoms and associated with defects.[35] The G/D band ratio observed in our samples, ∼19, indicates a

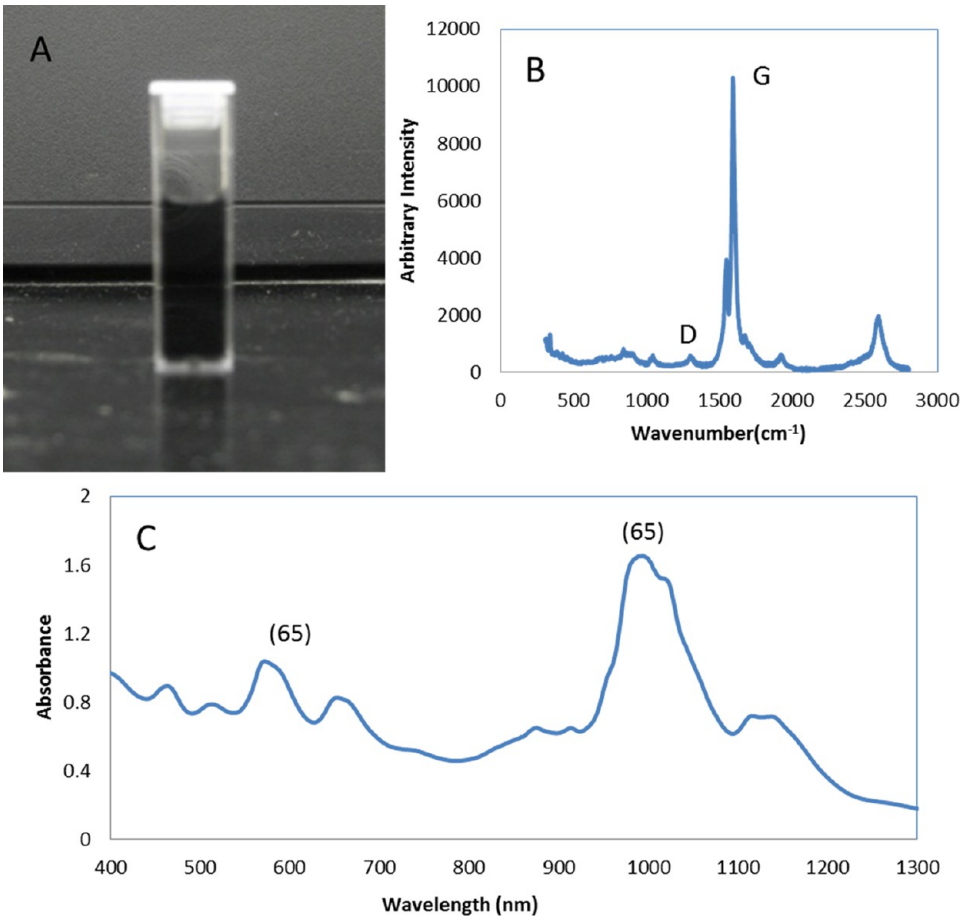

Figure 2. Picture of a cuvette containing an aqueous dispersion of SWNTs stabilized by SDBS surfactants (A). Representative Raman spectrum of dry SWNTs obtained after sonication (B). Representative UV−vis absorption spectrum of an aqueous SWNT dispersion (C). Highlighted are the peaks representative of the D and G bands in panel B, and those characteristic of (6,5) SWNTs in panel C.

dx.doi.org/10.1021/jp4039336 | J. Phys. Chem. B XXXX, XXX, XXX−XXX

low amount of impurities and imperfections in the SWNTs used for the present work.

Typical UV−vis absorption spectra obtained from our SWNT dispersions show peaks centered at ∼567 and ∼978 nm, characteristic of (6,5) SWNTs (see Figure 2C). The spectra obtained from our carbon nanotube dispersions guarantee that the majority of the SWNTs used in our experiments are (6,5). For the explanation of other peaks visible in Figure 2C please refer to data sheet for SG65i nanotubes provided by SWeNT in ref 41. Because the majority of SWNTs in the samples used in our experiments are (6,5), we only track the characteristic peaks for these SWNTs in the remainder of the paper.

3.3. Dialysis. In Figure 3 we provide pictures of the dialysis cells containing either W+SWNT (panels A1, A2, and A3) or LIPO+SWNT suspensions (panels B1, B2, and B3). Panels A1 and B1 are representative images of the samples as prepared, before the dialysis is initiated. The pictures in panels A2 and B2 are obtained on the fifth day of dialysis, and those in panels A3 and B3 are obtained for the dialysis membranes, without suspensions, at the end of the dialysis experiment.

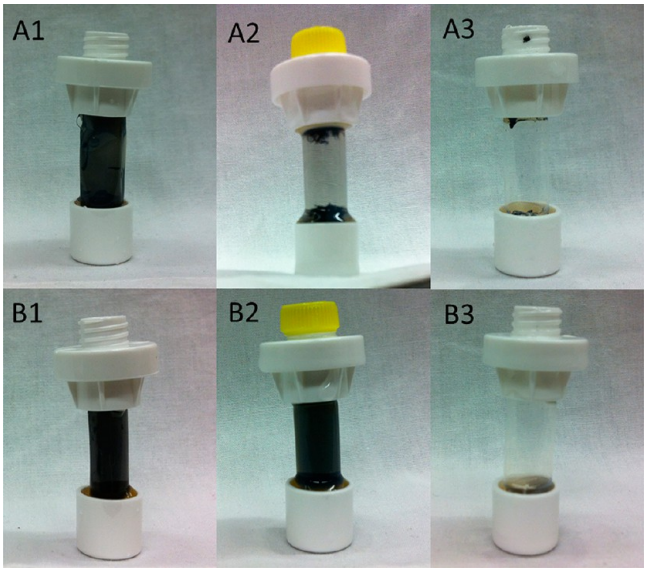

Figure 3. Pictures of W+SWNT (panels A1, A2, and A3) and LIPO+SWNT suspensions (panels B1, B2, and B3) before, during, and after dialysis, respectively. Panels A1 and B1 are for the two samples before dialysis. Pictures A2 and B2 are obtained on the fifth day of dialysis. Pictures A3 and B3 are for the empty dialysis cells at the end of the experiments. See section 2.4 for details on system composition.

Visual analysis of the results in panels A1 and B1 suggests that the two dispersions look similar to each other before dialysis. Analysis of panel A2 suggests the agglomeration of SWNTs from the W+SWNT sample on the fifth day of dialysis. No visible SWNTs agglomerates were observed in the first 4 days of dialysis for the W+SWNT system (data not shown because indistinguishable from those reported in Figure 3—note that quantification for this observation is obtained via the data shown in Figure 5, discussed below). Analysis of panel B2 suggests that the LIPO+SWNT suspension remains stable on the fifth day of dialysis. We found that the LIPO+SWNT suspension of Figure 3, panel B2, remained stable for about 1 month at ambient conditions without the formation of visible SWNTs agglomerates. Visual analysis of the dialysis cells at the end of the experiments (panels A3 and B3) suggests that there was no visible SWNT agglomerates deposited on the dialysis membranes. This was confirmed by Raman spectroscopy obtained for the membranes, which showed very weak signals in correspondence of the G band (data shown in Figure S3 of the Supporting Information).

We employed UV−vis spectroscopy to monitor the concentration of SWNTs, liposomes, and SDBS in the bulk water outside of the dialysis cell. The representative peaks are centered at ∼567 nm for (6,5) SWNTs,[35] at ∼205 nm for egg-PC,[42] and at ∼223 nm for SDBS.[43] We did not observe the characteristic absorbance of (6,5) SWNTs and egg-PCs in the bulk solution. This observation is consistent with the fact that the dialysis membranes do not allow either liposomes or SWNTs to diffuse out of the dialysis bag.

The concentration of SDBS in the bulk water can be determined by the maximum absorbance at 223 nm. We first obtained a standard calibration curve for SDBS concentration (data shown as Figure S4 in the Supporting Information). The calibration curve showed linearity up to the concentration of 0.06 mg/mL, which is consistent with the literature.[43] For all systems considered, except 4_LIPO+SWNT, the maximum SDBS concentration in the bulk water was estimated in 0.025 mg/mL, obtained when all SDBS used to stabilize the SWNTs diffused out of the dialysis cell. For the 4_LIPO+SWNT system, the maximum concentration in the bulk is expected to be ∼0.006 mg/mL. This guarantees that UV−vis SDBS absorbance in bulk water remains within the linear region of the calibration curve during our dialysis experiments.

In Figure 4, top panel, we report the absorbance at 223 nm in the bulk water as a function of time during our dialysis experiments. The SDBS concentration on the 10th day of dialysis for W+SDBS, W+SWNT, and LIPO+SWNT suspensions was found to be ∼0.025 mg/mL. For the 4_LIPO+SWNT system, the SDBS concentration in the bulk water after 10 days of dialysis was found to be ∼3/4 lower than that obtained for the other systems, which is a consequence of the lower amount of SDBS present in the suspension before the dialysis experiment (note that 1.25 mL was used for the 4_LIPO+SWNT system, while 2 mL was used for all other systems). In all cases, the SDBS concentration in the bulk increases linearly with time until a concentration of ∼90% of the maximum is reached, which occurs in the first ∼90 h of the experiment. The bulk SDBS concentration changes little after ∼100 h. These results suggest that most of the SDBS present within the various dialysis bags diffuses into the bulk solution during the first 4 days of dialysis.

In the bottom panel of Figure 4 we report the estimated SDBS concentration inside the dialysis cell as it decreases during dialysis. The results suggest that liposomes and/or SWNTs have limited effects on the diffusion of SDBS out of the dialysis cells, and that at ∼90 h the SDBS concentration within the dialysis cells is lower than the critical micelle concentration (cmc) of SDBS in water (∼0.7 mg/mL).[44]

As mentioned discussing Figure 3, we found that SWNTs dispersed in water by SDBS start agglomerating on the fifth day of dialysis. Combining this observation with the estimated SDBS concentration as a function of time, we conclude that SDBS surfactants are not effective at stabilizing SWNTs in water when their concentration is below the cmc. This is consistent with observations reported by Matarredona et al.[44] according to whom very little SDBS adsorbs on SWNTs below the surfactant cmc. The self-assembled aggregates predicted for

dx.doi.org/10.1021/jp4039336 | J. Phys. Chem. B XXXX, XXX, XXX−XXX

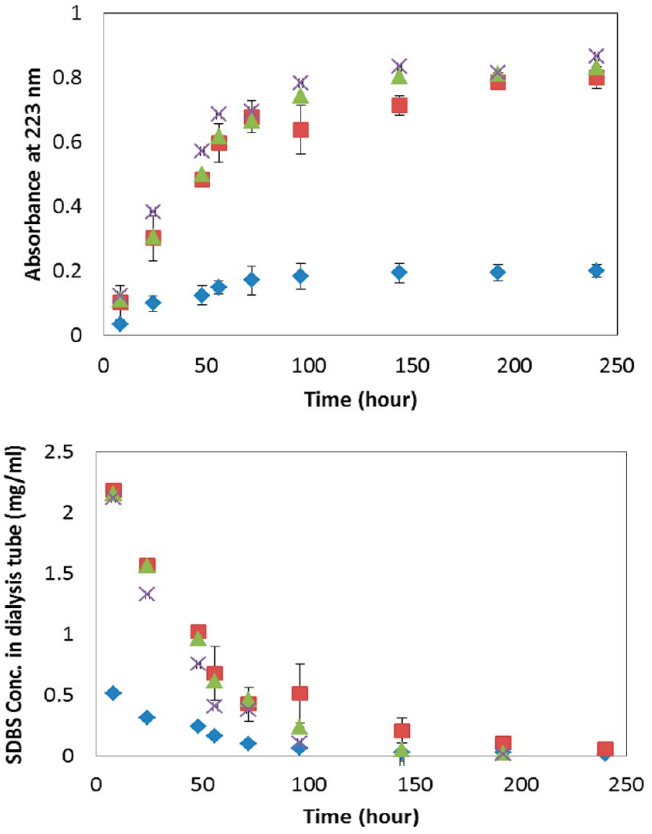

Figure 4. Absorbance at 223 nm in the bulk water during dialysis experiments (top panel) and estimated SDBS concentration inside the dialysis cell (bottom panel) as a function of time. Only representative error bars are reported for clarity. Different symbols represent data obtained for different systems. Green triangles are for W+SDBS suspensions, purple crosses for W+SWNT, red squares LIPO+SWNT, and blue diamonds 4_LIPO+SWNT. See section 2.4 for details on system composition.

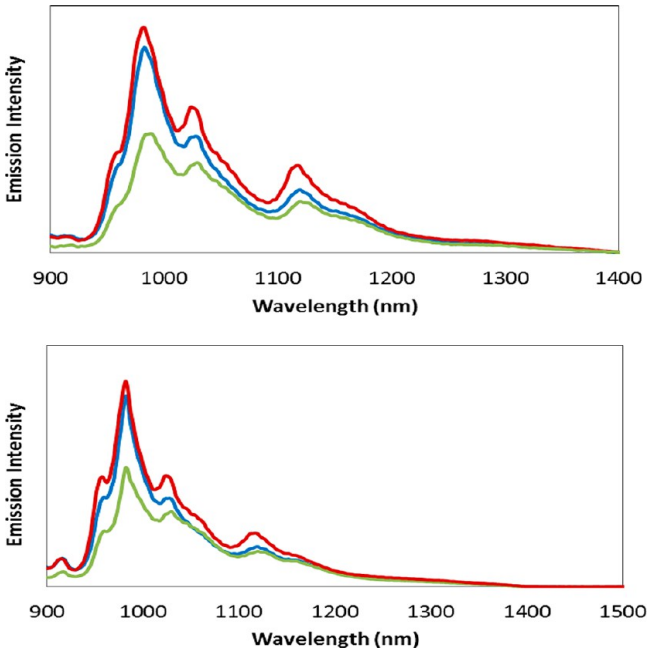

Figure 5. Fluorescence emission spectra for different SWNT dispersions. Blue lines are for the W+SWNT suspension before dialysis, purple for the LIPO+SWNT suspension before dialysis, green for the W+SWNT suspension on the fourth day of dialysis, and red for the LIPO+SWNT suspension on the fourth day of dialysis. Note that red and purple lines overlap, and hence are not distinguishable. The results are obtained from excitation lasers at 532 and 783 nm (top and bottom panel, respectively). See section 2.4 for system composition.

SDBS on SWNTs[35,45] can therefore form only at high bulk surfactant concentration. More importantly, because our results show that most SDBS has escaped the dialysis cell in all cases considered herein, the fact that SWNTs remain stable in the aqueous dispersions at conditions at which SDBS is not in enough concentration to prevent SWNTs agglomeration, our results for the LIPO+SWNT suspension suggest that the presence of liposomes can prevent SWNTs from agglomerating in water.

The intensity of the fluorescence emission can be used to quantify the dispersion quality of a SWNT suspension.[46,47] The fluorescence emission spectra from the W+SWNT and LIPO +SWNT samples are reported in Figure 5. The blue curve is from the W+SWNT sample before dialysis, which corresponds to the well-dispersed SWNT suspension. The fluorescence intensities from the W+SWNT sample on the fourth day of dialysis (green) are quenched by ~30% in comparison to those obtained from the same sample before dialysis. The results are consistent with a deterioration of the quality of the dispersion on the fourth day of dialysis, with the probable appearance of SWNTs aggregates large enough to be visible on the fifth day of dialysis. This observation suggests that a nucleation-and-growth process might be responsible for the formation of SWNT bundles within the W+SWNT sample at low SDBS concentration, because it takes a long time for the formation of the first small aggregates, but then the further deterioration of the dispersion seems to proceed quickly.

The fluorescence emission spectra obtained from the LIPO +SWNT dispersion on the fourth day of dialysis is similar to the one obtained for the same sample before dialysis (red and purple lines overlap in Figure 5 and are practically indistinguishable), indicating well-dispersed SWNTs in both suspensions. This confirms that the presence of liposomes prevents SWNTs from bundling, even at very low SDBS concentration.

While the mechanism by which SDBS surfactants stabilize carbon nanotube dispersions is understood, at least qualitatively (the surfactants adsorbed on the nanotubes provide effective nanotube−nanotube repulsive forces),[48] it remains to be understood how the liposomes stabilize the SWNTs dispersions. Egg-PC monomer is not efficient in dispersing SWNTs according to both literature[49,50] and our own experiments (not discussed at length for brevity; however, when we sonicated carbon nanotubes in the presence of egg-PC in aqueous systems at ambient conditions, visual inspection revealed the formation of bundles and carbon nanotube precipitation within minutes from the preparation). One very distinct possibility is that the liposomes adsorb onto SWNTs, thus preventing SWNTs agglomeration by steric resistance. For completeness, it should be clarified that the residual SDBS concentration after 4 days dialysis was estimated in ~0.025 mg/mL for the LIPO+SWNT suspension and ~0.006 mg/mL for the 4_LIPO+SWNT suspension. SWNTs agglomerates were observed in additional dialysis experiments in which we completely removed SDBS or reduced the concentration of liposomes compared to the systems discussed above. It appears that a minimum concentration of both SDBS and liposomes is

dx.doi.org/10.1021/jp4039336 | J. Phys. Chem. B XXXX, XXX, XXX−XXX

necessary to stabilize SWNTs in water. Because determining such limits is beyond the scopes of the present work, we do not discuss such experiments herein in more details.

Because the size of the liposomes used in the present study is much larger than the diameter of the nanotubes, it is also possible that the nanotubes adsorb onto the external surfaces of the liposomes. Thus, the apparent stability of the nanotube dispersion would be improved because of the effective liposome–liposome repulsion, although the nanotubes are not individually dispersed in the aqueous system. We also point out that our experiments were conducted for SWNTs from a single batch, with median length ~1.5 μm (as estimated by the manufacturer). Although nanotubes shorter than the median are present within the sample, it is possible that our results would change when nanotubes of different lengths are employed.

3.4. Freeze-Fracture TEM Characterization of Liposomes–SWNT Complexes. We employed freeze-fracture TEM to visualize complexes formed between liposomes and SWNTs. Representative TEM images of the replicas made from LIPO+SWNT suspensions collected on the fourth day of dialysis are shown in Figure 6. The TEM images corroborate

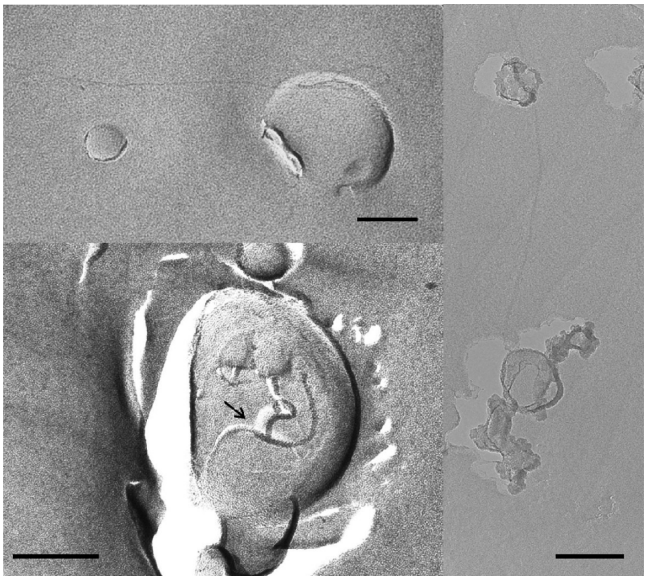

Figure 6. Freeze-fracture TEM images of the LIPO+SWNT suspension collected on the fourth day of dialysis. The dark area in the bottom left corner is caused by platinum accumulation during sample preparation. No platinum is present in the shadow (white) areas. The arrow highlights SWNTs. All the scale bars in the figure are 100 nm long.

our earlier interpretation, suggesting that liposomes can be found near and maybe adsorbed on the SWNTs in water at low SDBS concentration. In the bottom left of Figure 6 we highlight the linear dark and shadow (white) areas on the top surface of the liposome (marked by the arrow). The dark area is caused by platinum accumulation caused by the sample preparation. The shadow (white) area indicates that no platinum has accumulated in this region. Although there is no irrefutable evidence for the presence of nanotubes, we tentatively conclude that the linear shape highlighted is due to the presence of SWNTs on top of the liposome.

In the top left of Figure 6, the TEM image provides additional evidence concerning the structure of liposome–SWNT aggregates. In this case, the linear trace representative of the SWNT is due not to platinum accumulation, but to the carbon coating produced during the sample preparation. In the top right image, one SWNT is seen to interact simultaneously with two liposomes. It is important to point out that the diameter of the SWNTs cannot be easily determined from cryo-TEM images. Because of the accumulation of carbon and platinum on the replicas, the estimated diameters are generally larger than those of the true SWNTs. Thus, although the structures observed in Figure 6 appear as large as SWNTs bundles, based on their diameters, they can be small bundles and maybe even individual SWNTs.

The liposomes shown in Figure 6 as they interact with SWNTs are nearly spherical, suggesting the interaction with SWNTs does not significantly affect the liposome structure. Although the freeze-fracture TEM images cannot distinguish if SWNTs are located in or out of the liposomes, our hypothesis is that SWNTs adsorb on the surface of liposomes. This hypothesis is sustained by several observations. First of all, the SWNTs used in this work are too long to completely embed in the liposomes without piercing the phospholipid membranes. Second, if SWNTs are piercing the liposomes, they should affect the liposomes' shape, at least near the point of contact. Clearly, this is in conflict with our observations.

3.5. Dye-Leakage Experiments. To confirm that the SWNTs do not pierce the liposomes, we conducted dye-leakage experiments. Liposomes containing calcein were prepared for these experiments, as described in section 2.5. In Figure 7 we

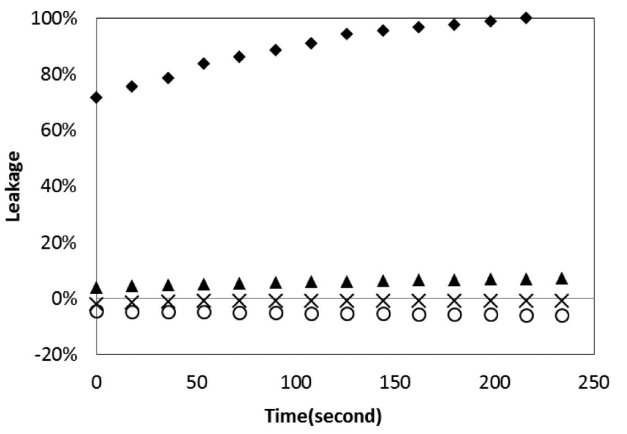

Figure 7. Calcein leakage from liposomes due to the addition of different reagents. Leakage data are expressed in percent of the leakage due to addition of Triton-100 surfactants, known to disrupt the liposomes (details in section 2.5). Data obtained upon addition of SDBS are represented by the filled triangles, those due to Triton-100 as filled diamonds; those due to the addition of a dispersion of SWNTs stabilized by SDBS are shown as crosses, and those obtained upon addition of a SWNT dispersion with low SDBS concentration as empty circles. Error bars are in most cases smaller than the symbols.

report the leakage of calcein within the first 4 min after adding different reagents to the liposome suspensions. The leakage data obtained in the presence of SWNTs start from negative values, because SWNTs absorb a certain amount of both excitation and emission lights and consequently the fluorescence intensities are lower than the one defined as 0% leakage.

The results show that when SDBS is added to the liposomes the % leakage increases slightly as the time increases, suggesting that SDBS increases the permeability of the liposome

dx.doi.org/10.1021/jp4039336 | J. Phys. Chem. B XXXX, XXX, XXX–XXX

membranes to calcein, probably by adsorbing within the membranes. We note, however, the leakage caused by SDBS is much less compared to the one measured when Triton X-100 is added to the liposomes. The addition of SWNTs dispersion also causes the liposomes to leak calcein over time. As the SWNTs are stabilized by SDBS (~5 mg/mL), it is possible that the leakage just described is due to SDBS−liposomes interactions. To support this possibility, we note that leakage data obtained in the presence of the SWNT dispersion are very similar to those obtained when SDBS solutions were added to the liposomes (compare crosses and triangles in Figure 7). We also point out that when a SWNT dispersion was used in which the SDBS concentration was reduced to ~0.4 mg/mL, leakage was less pronounced (empty circles in Figure 7). No obvious calcein leakage from the liposomes due to the addition of SWNTs suggests that the SWNTs do not affect the liposomes' permeability, which suggests they probably do not pierce the liposomes.

In a control experiment (shown in Figure S5 of the Supporting Information), we added Triton X-100 surfactants to one liposome−SWNT suspension that was dialyzed for 4 days. We found that Trion X-100 caused calcein leakage, indicating that the liposomes remained rather intact during the 4-day dialysis even in the presence of the SWNTs. This finding is consistent with our hypothesis that SWNTs, at the experimental conditions tested in our experiments, neither pierce nor strongly perturb the structure of the phospholipid liposome membranes.

Additional experiments, shown in Figure S6 of the Supporting Information, were performed using liposome samples in which the presence of multilamellar liposomes (diameter larger than 200 nm) was reduced as much as possible. These dispersions were prepared by extruding 20 times liposomes dispersions through a membrane with pores of diameter 200 nm. The liposomes so obtained were used in calcein-leakage experiments. These experiments were conducted to eliminate the possibility that SWNTs perturb the outer but not the inner lamellae of liposomes. Our results were consistent with those shown in Figure 7, further indicating that SWNTs do not severely disrupt liposomes, under the conditions considered herein.

4. DISCUSSION

The experiments discussed above confirm that SWNTs can be dispersed in aqueous systems at low ionic strength by the SDBS surfactant. When the SDBS concentration is reduced well below the critical micelle concentration, the SWNTs agglomerate into bundles.

When the SWNTs, stabilized by SDBS in aqueous systems at low ionic strength, come in contact with liposomes, our results do not show evidence of perturbation of the liposomes due to the CNTs. Instead, we find evidence of perturbation due to the SDBS surfactant, which could intercalate within the phospholipid membrane, altering its mechanical as well as barrier properties. Although this result is consistent with some literature observations,[51,52] it constitutes a significant step forward in our understanding of the interactions between CNTs and phospholipid membranes. In the remainder of the discussion, we put our results in relation to recent findings that may help rationalize our conclusions.

Hirano et al.[53] studied the influence of SWNTs conjugated with positively charged lysozyme on the leakage of negatively charged DOPC/DOPG liposomes. In agreement with our findings, they reported that SWNTs themselves cause very little leakage.

Posner and collaborators quantified the distribution of fullerene, titanium dioxide, and gold nanoparticles between lipid bilayers and water.[24,25] The findings show that the nanoparticles having positive surface charge yield pronounced dye leakages from negatively charged PC liposomes irrespective of the nanoparticle core composition. Negatively charged nanoparticles showed a less pronounced dye leakage. These results suggest that electrostatic interactions are among the critical factors that determine the perturbation of a liposome. In our experiments, the SWNTs are partially covered by the negatively charged SDBS surfactants. This might explain, in part, the little perturbation produced by the SWNTs on the negatively charged liposomes. Comparing our results to those just mentioned from the literature suggests that perhaps carbon nanotubes much shorter than the ones used in the present work might lead to different results.

Mecke et al.[26] reported that polymeric nanoparticles with a diameter between 8 and 10 nm cause the formation and growth of holes in model membranes, whereas nanoparticles of diameter 6 nm or less yield minor disruptions on the lipid bilayer. Leroueil et al.[54] showed that 2 nm gold nanoparticles disrupt lipid bilayers primarily by aggregating near pre-existing defects, while 50 nm silica nanoparticles with the same surface functionality are capable of creating holes on the lipid bilayers. Moghadam et al.[55] found similar results for gold nanoparticles of size 10−20 nm. Cho et al. reported that the sedimentation of large nanoparticles can lead to a greater cellular uptake.[56] Because the SWNTs used in this work have diameter of ~0.8 nm, it is possible that they slightly affect the liposome membranes because of the limited interaction area between SWNTs and liposomes. Larger CNTs might have more pronounced effects.

Mutlu et al.[57] found that the toxicity of SWNTs was attributable to their aggregation rather than individual SWNTs. Although it is not clear that the disruption of cell membranes is the mechanism responsible for the SWNTs cytotoxicity, our results provide a potential explanation for the observation of Mutlu et al., according to which highly dispersed SWNTs with small diameter have limited effects on the perturbation of cell membranes.

Finally, it should be pointed out that our results suggest that liposomes could be used to stabilize SWNTs, provided that a small amount of SDBS surfactant is available and that the ionic strength of the aqueous system is maintained low. Because our data suggest that the liposomes at most adsorb on the SWNTs surfaces without undergoing significant restructuring of their phospholipid membranes, our data suggest a new mechanism that could be used to stabilize CNT dispersions for various applications. More studies need to be conducted to assess how this mechanism compares to existing technologies (e.g., dispersion stabilization using DNA, amino acids, polypeptides, or proteins adsorbed onto SWNTs).

5. CONCLUSIONS

We studied the interaction between SWNTs and liposome membranes via dialysis, freeze-fracture TEM, and dye-leakage experiments. Characterization experiments were performed using UV−vis, Raman, and fluorescence spectroscopies. The results from freeze-farcture TEM show that SWNTs interact with liposomes in water, possibly by adsorbing on to phospholipid bilayers. Liposomes remain spherical, suggesting

that the interaction does not alter the liposomes structure. No obvious dye leakage is found upon the addition of SWNTs to liposome suspensions, suggesting that the perturbation of phospholipid bilayer caused by SWNTs is minor. The integrity of the phospholipid bilayers could be due to the repulsive electrostatic interactions between the residual SDBS surfactant on the SWNTs and the negatively charged liposomes, as well as to the small contact area between liposomes and SWNTs. We observed that SWNT dispersions in aqueous systems at low ionic strength are more stable in the presence than in the absence of liposomes at a low SDBS concentration under gentle shaking.

■ ASSOCIATED CONTENT

Ⓢ Supporting Information

Details of characterization data for liposomes dispersions, surfactant solutions, carbon nanotube dispersions, and additional dye-leakage experiments are provided. This material is available free of charge via the Internet at http://pubs.acs.org..

■ AUTHOR INFORMATION

Corresponding Author

*Phone: 1 405 325 5716. Fax: 1 405 325 5813. E-mail: astriolo@ou.edu.

Notes

The authors declare no competing financial interest.

■ ACKNOWLEDGMENTS

This work was supported, in part, by the U.S. National Science Foundation, under Award No. CBET-0853759.

■ REFERENCES

(1) Bianco, A. Carbon nanotubes for the *delivery* of therapeutic molecules. *Expert Opin. Drug Deliv.* **2004**, *1*, 57−65.

(2) Kostarelos, K.; Bianco, A.; Prato, M. Promises, facts and challenges for carbon nanotubes in imaging and therapeutics. *Nat. Nanotechnol.* **2009**, *4*, 627−633.

(3) Singh, R.; Pantarotto, D.; McCarthy, D.; Chaloin, O.; Hoebeke, J.; Partidos, C. D.; Briand, J.-P.; Prato, M.; Bianco, A.; Kostarelos, K. Binding and condensation of plasmid DNA onto functionalized carbon nanotubes: toward the construction of nanotube-based gene delivery vectors. *J. Am. Chem. Soc.* **2005**, *127*, 4388−4396.

(4) Podesta, J. E.; Al-Jamal, K. T.; Herrero, M. A.; Tian, B.; Ali-Boucetta, H.; Hegde, V.; Bianco, A.; Prato, M.; Kostarelos, K. Antitumor activity and prolonged survival by carbon-nanotube-mediated therapeutic siRNA silencing in a human lung xenograft model. *Small* **2009**, *5*, 1176−1185.

(5) Kam, N. W. S.; Liu, Z.; Dai, H. Carbon nanotubes as intracellular transporters for proteins and DNA: an investigation of the uptake mechanism and pathway. *Angew. Chem., Int. Ed. Engl.* **2006**, *45*, 577−581.

(6) Samori, C.; Ali-Boucetta, H.; Sainz, R.; Guo, C.; Toma, F. M.; Fabbro, C.; da Ros, T.; Prato, M.; Kostarelos, K.; Bianco, A. Enhanced anticancer activity of multi-walled carbon nanotube-methotrexate conjugates using cleavable linkers. *Chem. Commun. (Camb.)* **2010**, *46*, 1494−1496.

(7) Wu, W.; Wieckowski, S.; Pastorin, G.; Benincasa, M.; Klumpp, C.; Briand, J.-P.; Gennaro, R.; Prato, M.; Bianco, A. Targeted delivery of amphotericin B to cells by using functionalized carbon nanotubes. *Angew. Chem., Int. Ed. Engl.* **2005**, *44*, 6358−6362.

(8) Zhu, Y.; Ran, T.; Li, Y.; Guo, J.; Li, W. Dependence of the cytotoxicity of multi-walled carbon nanotubes on the culture medium. *Nanotechnology* **2006**, *17*, 4668−4674.

(9) Kostarelos, K.; Lacerda, L.; Pastorin, G.; Wu, W.; Wieckowski, S.; Luangsivilay, J.; Godefroy, S.; Pantarotto, D.; Briand, J.-P.; Muller, S.; et al. Cellular uptake of functionalized carbon nanotubes is independent of functional group and cell type. *Nat. Nanotechnol.* **2007**, *2*, 108−113.

(10) Al-Jamal, K. T.; Nerl, H.; Muller, K. H.; Ali-Boucetta, H.; Li, S.; Haynes, P. D.; Jinschek, J. R.; Prato, M.; Bianco, A.; Kostarelos, K.; et al. Cellular uptake mechanisms of functionalised multi-walled carbon nanotubes by 3D electron tomography imaging. *Nanoscale* **2011**, *3*, 2627−2635.

(11) Shvedova, A.; Castranova, V.; Kisin, E.; Schwegler-Berry, D.; Murray, A.; Gandelsman, V.; Maynard, A.; Baron, P. Exposure to carbon nanotube material: assessment of nanotube cytotoxicity using human keratinocyte cells. *J. Toxicol. Environ. Health A* **2003**, *66*, 1909−1926.

(12) Manna, S. K.; Sarkar, S.; Barr, J.; Wise, K.; Barrera, E. V.; Jejelowo, O.; Rice-Ficht, A. C.; Ramesh, G. T. Single-walled carbon nanotube induces oxidative stress and activates nuclear transcription factor-kappaB in human keratinocytes. *Nano Lett.* **2005**, *5*, 1676−1684.

(13) Lam, C.-W.; James, J. T.; McCluskey, R.; Hunter, R. L. Pulmonary toxicity of single-wall carbon nanotubes in mice 7 and 90 days after intratracheal instillation. *Toxicol. Sci.* **2004**, *77*, 126−134.

(14) Chen, X.; Tam, U. C.; Czlapinski, J. L.; Lee, G. S.; Rabuka, D.; Zettl, A.; Bertozzi, C. R. Interfacing carbon nanotubes with living cells. *J. Am. Chem. Soc.* **2006**, *128*, 6292−6293.

(15) Dumortier, H.; Lacotte, S.; Pastorin, G.; Marega, R.; Wu, W.; Bonifazi, D.; Briand, J.-P.; Prato, M.; Muller, S.; Bianco, A. Functionalized carbon nanotubes are non-cytotoxic and preserve the functionality of primary immune cells. *Nano Lett.* **2006**, *6*, 1522−1528.

(16) Wick, P.; Manser, P.; Limbach, L. K.; Dettlaff-Weglikowska, U.; Krumeich, F.; Roth, S.; Stark, W. J.; Bruinink, A. The degree and kind of agglomeration affect carbon nanotube cytotoxicity. *Toxicol. Lett.* **2007**, *168*, 121−131.

(17) Crouzier, T.; Nimmagadda, A.; Nollert, M. U.; McFetridge, P. S. Modification of single walled carbon nanotube surface chemistry to improve aqueous solubility and enhance cellular interactions. *Langmuir* **2008**, *24*, 13173−13181.

(18) Kang, S.; Herzberg, M.; Rodrigues, D. F.; Elimelech, M. Antibacterial effects of carbon nanotubes: size does matter! *Langmuir* **2008**, *24*, 6409−6413.

(19) Vecitis, C. D.; Zodrow, K. R.; Kang, S.; Elimelech, M. Electronic-structure-dependent bacterial cytotoxicity of single-walled carbon nanotubes. *ACS Nano* **2010**, *4*, 5471−5479.

(20) Porter, A. E.; Gass, M.; Bendall, J. S.; Muller, K.; Goode, A.; Skepper, J. N.; Midgley, P. A.; Welland, M. Uptake of noncytotoxic acid-treated single-walled carbon nanotubes into the cytoplasm of human macrophage cells. *ACS Nano* **2009**, *3*, 1485−1492.

(21) Singh, P.; Samori, C.; Toma, F. M.; Bussy, C.; Nunes, A.; Al-Jamal, K. T.; Menard-Moyon, C.; Prato, M.; Kostarelos, K.; Bianco, A. Polyamine functionalized carbon nanotubes: synthesis, characterization, cytotoxicity and siRNA binding. *J. Mater. Chem.* **2011**, *21*, 4850−4860.

(22) Liu, S.; Wei, L.; Hao, L.; Fang, N.; Chang, M. W.; Xu, R.; Yang, Y.; Chen, Y. Sharper and faster "nano darts" kill more bacteria: a study of antibacterial activity of individually dispersed pristine single-walled carbon nanotube. *ACS Nano* **2009**, *3*, 3891−3902.

(23) Vácha, R.; Martinez-Veracoechea, F. J.; Frenkel, D. Receptor-mediated endocytosis of nanoparticles of various shapes. *Nano Lett.* **2011**, *11*, 5391−5395.

(24) Hou, W.-C.; Moghadam, B. Y.; Corredor, C.; Westerhoff, P.; Posner, J. D. *Environmental* Distribution of functionalized gold nanoparticles between water and lipid bilayers as model cell membranes. *Environ. Sci. Technol.* **2012**, *46*, 1869−1876.

(25) Hou, W.-C.; Moghadam, B. Y.; Westerhoff, P.; Posner, J. D. Distribution of fullerene nanomaterials between water and model biological membranes. *Langmuir* **2011**, *27*, 11899−11905.

(26) Mecke, A.; Majoros, I. J.; Patri, A. K.; Baker, J. R.; Banaszak Holl, M. M.; Orr, B. G. Lipid bilayer disruption by polycationic polymers: the roles of size and chemical functional group. *Langmuir* **2005**, *21*, 10348−10354.

(27) Karchemski, F.; Zucker, D.; Barenholz, Y.; Regev, O. Carbon nanotubes-liposomes conjugate as a platform for drug delivery into cells. *J. Controlled Release* **2012**, *160*, 339−345.
(28) Wallace, E. J.; Sansom, M. S. P. Blocking of carbon nanotube based nanoinjectors by lipids: a simulation study. *Nano Lett.* **2008**, *8*, 2751−2756.
(29) Höfinger, S.; Melle-Franco, M.; Gallo, T.; Cantelli, A.; Calvaresi, M.; Gomes, J. A. N. F.; Zerbetto, F. A computational analysis of the insertion of carbon nanotubes into cellular membranes. *Biomaterials* **2011**, *32*, 7079−7085.
(30) Parthasarathi, R.; Tummala, N. R.; Striolo, A. Embedded single-walled carbon nanotubes locally perturb DOPC phospholipid bilayers. *J. Phys. Chem. B* **2012**, *116*, 12769−12782.
(31) Ghosh, S.; Bachilo, S. M.; Weisman, R. B. Advanced sorting of single-walled carbon nanotubes by nonlinear density-gradient ultracentrifugation. *Nat. Nanotechnol.* **2010**, *5*, 443−450.
(32) Forlow, S. B.; McEver, R. P.; Nollert, M. U. Leukocyte-leukocyte interactions mediated by platelet microparticles under flow. *Blood* **2000**, *95*, 1317−1323.
(33) Yamaguchi, T.; Nomura, M.; Matsuoka, T.; Koda, S. Effects of frequency and power of ultrasound on the size reduction of liposome. *Chem. Phys. Lipids* **2009**, *160*, 58−62.
(34) Ilker, M. F.; Nüsslein, K.; Tew, G. N.; Coughlin, E. B. Tuning the hemolytic and antibacterial activities of amphiphilic polynorbornene derivatives. *J. Am. Chem. Soc.* **2004**, *126*, 15870−15875.
(35) Tan, Y.; Resasco, D. E. Dispersion of single-walled carbon nanotubes of narrow diameter distribution. *J. Phys. Chem. B* **2005**, *109*, 14454−14460.
(36) Bachilo, S. M.; Balzano, L.; Herrera, J. E.; Pompeo, F.; Resasco, D. E.; Weisman, R. B. Narrow (*n*,*m*)-Distribution of Single-Walled Carbon Nanotubes Grown Using a Solid Supported Catalyst. *J. Am. Chem. Soc.* **2003**, *125*, 11186−11187.
(37) Bachilo, S. M.; Strano, M. S.; Kittrell, C.; Hauge, R. H.; Smalley, R. E.; Weisman, R. B. Structure-Assigned Optical Spectra of Single-Walled Carbon Nanotubes. *Science* **2002**, *298*, 2361−2366.
(38) Siitonen, A. J.; Tsyboulski, D. A.; Bachilo, S. M.; Weisman, R. B. Surfactant-Dependent Exciton Mobility in Single-Walled Carbon Nanotubes Studied by Single-Molecule Reactions. *Nano Lett.* **2010**, *10*, 1595−1599.
(39) Silvera-Batista, C. A.; Wang, R. K.; Weinberg, P.; Ziegler, K. J. Solvatochromic shifts of single-walled carbon nanotubes in nonpolar microenvironments. *Phys. Chem. Chem. Phys.* **2010**, *12*, 6990−6998.
(40) Suttipong, M.; Tummala, N. R.; Striolo, A.; Silvera Batista, C.; Fagan, J. Salt-Specific Effects in Aqueous Dispersions of Carbon Nanotubes. *Soft Matter* **2013**, *9*, 3712−3719.
(41) http://www.swentnano.com/tech/docs/SG65i_Data_Sheet.pdf.
(42) Maskrey, B. H.; Bermúdez-Fajardo, A.; Morgan, A. H.; Stewart-Jones, E.; Dioszeghy, V.; Taylor, G. W.; Baker, P. R. S.; Coles, B.; Coffey, M. J.; Kühn, H.; et al. Activated platelets and monocytes generate four hydroxyphosphatidylethanolamines via lipoxygenase. *J. Biol. Chem.* **2007**, *282*, 20151−20163.
(43) Pedersen, K. H.; Andersen, S. I.; Jensen, A. D.; Dam-Johansen, K. Replacement of the foam index test with surface tension measurements. *Cem. Concr. Res.* **2007**, *37*, 996−1004.
(44) Matarredona, O.; Rhoads, H.; Li, Z.; Harwell, J. H.; Balzano, L.; Resasco, D. E. Dispersion of Single-Walled Carbon Nanotubes in Aqueous Solutions of the Anionic Surfactant NaDDBS. *J. Phys. Chem. B* **2003**, *107*, 1335713367.
(45) Suttipong, M.; Tummala, N. R.; Kitiyanan, B.; Striolo, A. Role of Surfactant Molecular Structure on Self-Assembly: Aqueous SDBS on Carbon Nanotubes. *J. Phys. Chem. C* **2011**, *115*, 17286−17296.
(46) Runtang, W.; Paul, C.; Juan, G. D.; Tonya, K. L.; Melinda, K. L.; Christine, H. M.; Valerie, C. M.; Jodie, L. C.; Richard, E. S.; Howard, K. S.; et al. SWCNT PEG-eggs: Single-walled carbon nanotubes in biocompatible shell-crosslinked micelles. *Carbon* **2007**, *45*, 2388−2393.
(47) Ying, T.; Marina, Y. T.; Matti, P.; Albert, G. N.; Hua, J.; Zhen, Z.; Esko, I. K. Growth of single-walled carbon nanotubes with controlled diameters and lengths by an aerosol method. *Carbon* **2011**, *49*, 4636−4643.
(48) Tummala, N. R.; Morrow, B. H.; Resasco, D. E.; Striolo, A. Stabilization of Aqueous Carbon Nanotube Dispersions using Surfactants: Insights from Molecular Dynamics Simulations. *ACS Nano* **2010**, *4*, 7193−7204.
(49) Richard, C.; Balavoine, F.; Schultz, P.; Ebbesen, T. W.; Mioskowski, C. Supramolecular self-assembly of lipid derivatives on carbon nanotubes. *Science* **2003**, *300*, 775−778.
(50) Wu, Y.; Hudson, J. S.; Lu, Q.; Moore, J. M.; Mount, A. S.; Rao, A. M.; Alexov, E.; Ke, P. C. Coating single-walled carbon nanotubes with phospholipids. *J. Phys. Chem. B* **2006**, *110*, 2475−2478.
(51) Qy, X. Y.; Jiang, J. G. Toxicity evaluation of two typical surfactants to Dunaliella bardawil, an environmentally tolerant alga. *Environ. Toxicol. Chem.* **2013**, *32*, 426−433.
(52) Marcelino, J.; Lima, J. L.; Reis, S.; Matos, C. Assessing the effects of surfactants on the physical properties of liposome membranes. *Chem. Phys. Lipids* **2007**, *146*, 94−103.
(53) Hirano, A.; Uda, K.; Maeda, Y.; Akasaka, T.; Shiraki, K. One-dimensional protein-based nanoparticles induce lipid bilayer disruption: carbon nanotube conjugates and amyloid fibrils. *Langmuir* **2010**, *26*, 17256−17259.
(54) Leroueil, P. R.; Berry, S. A.; Duthie, K.; Han, G.; Rotello, V. M.; McNerny, D. Q.; Baker, J. R.; Orr, B. G.; Banaszak Holl, M. M. Wide varieties of cationic nanoparticles induce defects in supported lipid bilayers. *Nano Lett.* **2008**, *8*, 420−424.
(55) Moghadam, B. Y.; Hou, W.-C.; Corredor, C.; Westerhoff, P.; Posner, J. D. Role of nanoparticle surface functionality in the disruption of model cell membranes. *Langmuir* **2012**, *28*, 16318−16326.
(56) Cho, E. C.; Zhang, Q.; Xia, Y. The effect of sedimentation and diffusion on cellular uptake of gold nanoparticles. *Nat. Nanotechnol.* **2011**, *6*, 385−391.
(57) Mutlu, G. k. M.; Budinger, G. R. S.; Green, A. A.; Urich, D.; Soberanes, S.; Chiarella, S. E.; Alheid, G. F.; McCrimmon, D. R.; Szleifer, I.; Hersam, M. C. Biocompatible nanoscale dispersion of single-walled carbon nanotubes minimizes in vivo pulmonary toxicity. *Nano Lett.* **2010**, *10*, 1664−1670.